Nickel-Catalyzed Three-Component Cycloadditions of Enoates, Alkynes, and Aldehydes

Aireal D. Jenkins#, Michael T. Robo#, Paul M. Zimmerman,* and John Montgomery*

(# denotes equal contributors to this work)

Department of Chemistry, University of Michigan, 930 N. University Ave., Ann Arbor, MI, 48109-1055, USA.

paulzim@umich.edu

jmontg@umich.edu

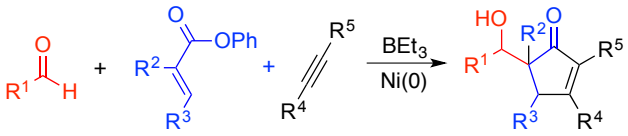

ABSTRACT: A method for the three-component cycloaddition of enoates, alkynes, and aldehydes has been developed. Building upon previous work by this group in which stoichiometrically generated metallacycles undergo alkylation, we report a catalytic, alkylative [3+2] cycloaddition. From simple starting materials, structurally complex cyclopentenones may be rapidly assembled. Computational investigation of the mechanism (ωB97X-D3/cc-pVTZ // ωB97X/6-31G(d)) identified three energetically feasible pathways. Based on the relative rates of ketene formation compared to isomerization to a 7-membered metallacycle, the most likely mechanism has been determined to occur "ketene-first", with carbocyclization prior to aldol addition. Deuterium labeling studies suggest that formation of the 7-membered metallacycle becomes possible when an α-substituted enoate is used. This observed change in selectivity is due to the increased difficulty of phenoxide elimination with the inclusion of additional steric

bulk of the α-substituent. The net transformation results in a [3+2] cycloaddition accompanied by an alkylation of the enoate substituent.

Introduction

Methods for enabling [3+2] cycloadditions typically involve 1,3-dipolar cycloadditions,[1] cyclopropane ring openings,[2] vinyl carbenoid additions,[3] cycloadditions of allyl, allenyl, or propargylsilanes accompanied by 1,2 silicon shifts,[4] or organocatalytic processes accompanied by a 1,2 hydrogen transfer.[5] As a complement to methods of this type, a number of metal-promoted processes have been developed utilizing the formal reductive [3+2] cycloaddition of α,β-unsaturated carbonyl derivatives with alkynes or allenes. By pairing a net two-electron reduction with the cycloaddition process, simple, readily available substrates may be utilized in the generation of five-membered carbocyclic ring systems. Early illustrations of reductive cycloadditions involved the stoichiometric generation of titanium,[6] nickel,[7] or iron metalacycles,[8] followed by either protonation or alkylation of a metal enolate motif. During processes of this type, the protonation or alkylation occurs on the enoate or enal α-carbon (Scheme 1). In the stoichiometric nickel processes involving alkylation of the intermediate metalacycle, a broad range of electrophiles were utilized,[7c] including aldehydes, alkyl halides, acyl chlorides, and enals as Michael acceptors. These alkylative processes, however, were restricted to intramolecular versions to enable synthesis of the well-defined metalacyclic species involved in the couplings.

Scheme 1. Reductive Cycloaddition Methods

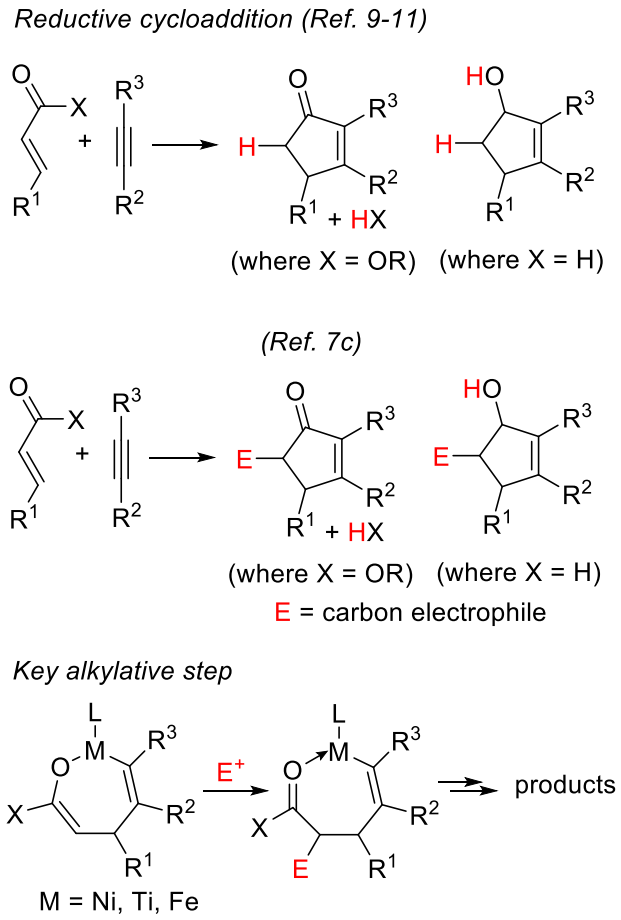

Catalytic versions of [3+2] reductive cycloadditions of enals and alkynes became possible with nickel catalysis by employing CH_3OH and Et_3B as a key reagent combination.[9] Methods involving enoate-alkyne cycloadditions utilizing either Et_3B or isopropanol as the terminal reductant then provided direct access to cyclopentenone products, and other types of nickel-catalyzed reductive cycloadditions have more recently been reported.[10] Following this work, a highly attractive enantio- and regioselective reductive cycloaddition process was developed, providing access to highly enantioenriched products,[11a] and other types of highly attractive and versatile nickel-catalyzed reductive cycloadditions have been developed using dihaloprecursors.[11b-d] Cobalt-catalyzed enone-allene cycloadditions provided a complementary

outcome with access to products possessing an exocyclic double bond.[12a] The cobalt-catalyzed method was further extended with access to [3.2.1] bicyclooctene products derived from cycloaddition of cyclic enones with alkynes.[12b] Hydrogen-mediated reductive cycloadditions of unsaturated carbonyls with two equivalents of acetylene allowed six-membered ring construction by a novel [2+2+2] pathway utilizing rhodium catalysis.[13] The above advances in catalytic reductive cycloaddition processes demonstrate the utility of the strategy in numerous contexts. However, alkylative versions, where a carbon electrophile is introduced to the enoate or enal α-position, have remained elusive since the initial demonstrations utilizing stoichiometrically-generated metalacycles.[7c] Herein, this void is addressed by the development of catalytic, alkylative [3+2] cycloadditions involving an aldol addition reaction as the key metalacycle alkylation step.

Results and Discussion

Discovery and Optimization. In our previous report of reductive cycloadditions of phenyl enoates with alkynes,[10a] a catalyst prepared from $Ni(COD)_2$ with PBu_3 allowed efficient enoate-alkyne reductive cycloaddition utilizing Et_3B as the reductant with 2% methanol in THF. By replacing methanol with benzaldehyde and conducting the reaction in toluene, catalytic alkylative cycloaddition was observed (Table 1, entry 1). In efforts to optimize the yield and diastereoselectivity of this process, reactions with PBu_3 were compared against a number of *N*-heterocyclic carbene (NHC) ligands with a wide range of steric properties. Yields were very poor with the unhindered NHC's IPrBAC and ITol (Table 1, entries 2-3), whereas IMes as ligand (Table 1, entry 4) afforded comparable yields with slightly lower selectivities compared to PBu_3. Yields were best with the bulkier ligand IPr, whereas the saturated analogue SIPr led to lower chemical yield (Table 1, entries 5-6). Notably, with both of these bulkier ligands IPr and SIPr, a reversal of

regiochemistry was noted compared with the outcome using PBu_3 or IMes. Stereochemical relationships of **1a** and **1b** were established by stereoselective Luche reduction and acetonide formation, followed by analysis of coupling constants and nOe relationships on the bicyclic derivatives.

Table 1. Ligand Optimization in Three-Component Cycloadditions

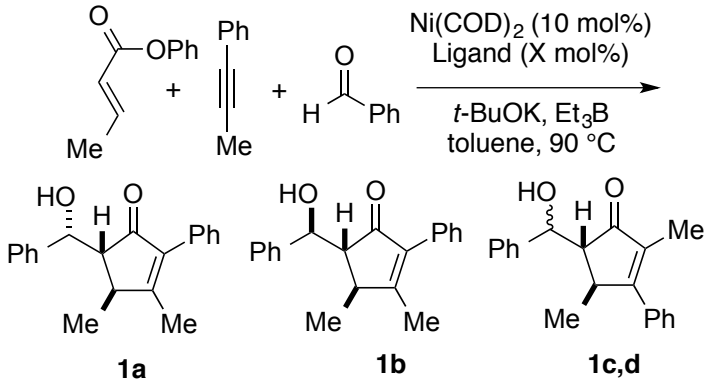

entry	ligand	X mol %	% yield[a]	**1a**:**1b**:**1c**:**1d**
1	PBu_3	20	57	69:26:5:0
2	IPrBAC•HCl	10	5	67:22:7:4
3	ITol•HCl	10	10	78:20:0:2
4	IMes•HCl	10	61	45:35:20:0
5	IPr•HCl	10	62	18:11:53:18
6	SIPr•HCl	10	36	12:3:64:23

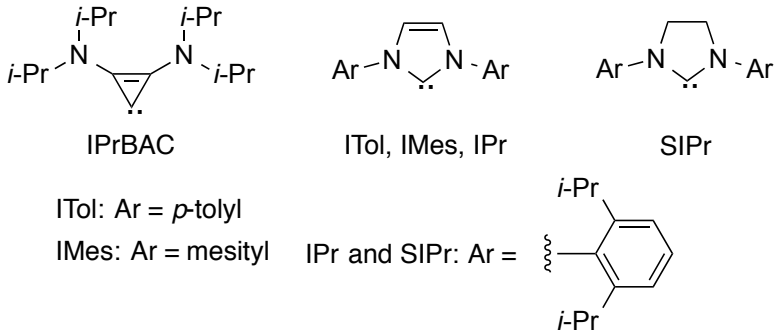

[a]Combined yield of the products **1a-1d.**

Exploration of the Substrate Scope. The scope of the three-component couplings was then expanded to include a range of enoate-alkyne-aldehyde combinations. While the PBu_3- and IMes-promoted procedures described above were satisfactory for some substrate combinations, in some instances, the reductive cycloaddition products (without aldehyde incorporation) were significant byproducts. In these cases, adding the enoate, alkyne, and Et_3B by syringe drive to a mixture of the catalyst and aldehyde served to minimize these byproducts and improve product yields. Additionally, precise assessment of inherent aldol diastereoselectivities was made difficult by the formation of small amounts of aldol elimination products. The alkylative cycloadditions of phenyl acrylate, lacking a β-substituent, was a representative case where slow addition of the enoate, alkyne, and reductant resulted in yield improvements (Scheme 2). Using IMes as ligand, the Et_3B-mediated cycloaddition of phenyl acrylate, phenyl propyne, and benzaldehyde proceeded in 35 % isolated yield when all components were added at once, whereas the yield improved to 48 % isolated yield (3:1 dr) of products **2a** and **2b** when the enoate, alkyne, and Et_3B reductant were added by syringe drive to a mixture of the Ni-IMes catalyst and benzaldehyde. In this case, only trace quantities of the minor regioisomer were detected.

Scheme 2. Slow Addition Protocol with Phenyl Acrylate

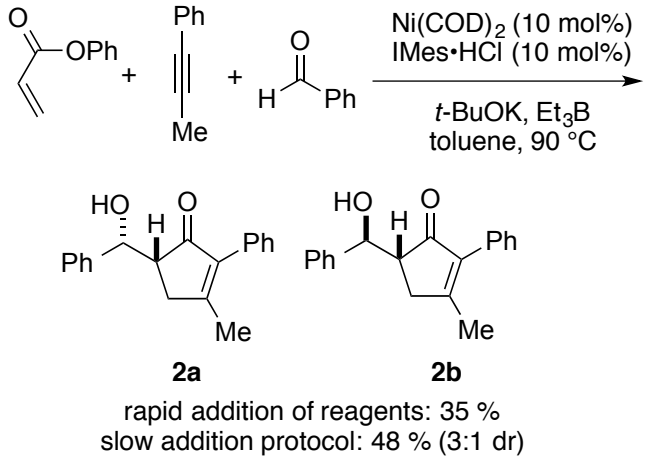

rapid addition of reagents: 35 %
slow addition protocol: 48 % (3:1 dr)

Based on the above observations, three general procedures were utilized in other cycloaddition attempts: procedure A involves PBu_3 as ligand, procedure B involves IMes as ligand, and procedure C involves IMes as ligand with slow addition of the enoate, alkyne, and Et_3B. The use of PBu_3 as ligand (procedure A) typically provided the highest selectivity favoring the major regioisomer, whereas the use of IMes as ligand (procedure B) provided improvements in chemical yield at the expense of selectivity. The slow addition protocol (procedure C) provided only marginal improvements in most cases; however, two cases with a fully unsubstituted phenyl enoate or β-aryl enoate showed moderate improvements compared with the analogous procedure without syringe drive addition. The following examples describe the optimal procedure, in some cases comparing two of the protocols examined when comparable results were obtained.

The optimal outcomes of previously described couplings (Table 1 and Scheme 2) are summarized as the examples where the three general procedures were developed (Table 2, entries 1-3). α-Substitution of the enoate was tolerated with either PBu_3 or IMes as ligand, with slightly better diastereoselectivity being observed with PBu_3 (Table 2, entries 4-5). A β-aryl substituted enoate was incorporated most efficiently using the syringe drive protocol of procedure C (Table 2,

entry 6). Additional examples demonstrated breadth of the method by examining non-aromatic internal alkynes (Table 2, entry 7), an aliphatic aldehyde (Table 2, entry 8), and alkynes bearing silyloxy or ester functionality (Table 2, entries 9-10). The *trans* relative configuration of the cyclopentenone ring substituents was directly established by nOe analysis for the major products of the catalytic cycloadditions. In several representative cases (entries 1, 3, 6, and 8), the side chain stereochemistry was determined through ketone reduction and acetonide formation followed by nOe analysis. The relative configurations were consistent aside from the product derived from an aliphatic aldehyde (Table 2, entry 8), where the major product was epimeric at the secondary hydroxyl compared with all other examples.

Table 2. Scope of Three-Component Cycloadditions

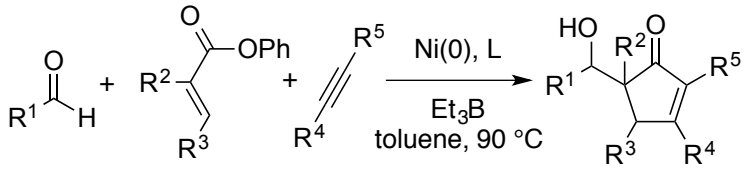

entry	procedure[a]	% yield[b]	isomer ratio[c]	major product[d]
1	A	57	69:26:5	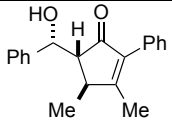
2	B	61	45:35:20	
3	C	48	69:25:6	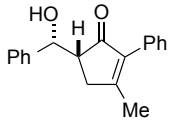
4	A	54	61:39	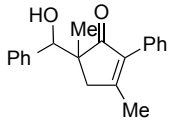
5	B	50	52:36:11	

6	C	50	65:29:6	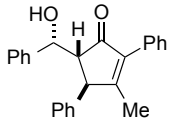
7	B	52	58:42	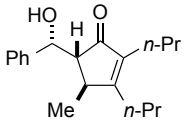
8	A	52	63:37	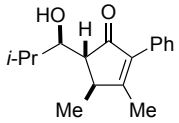
9	B	57	54:37:9	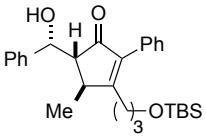
10	B	47	54:33:13	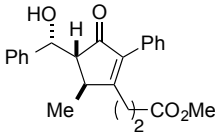

[a] Procedure A utilizes $Ni(COD)_2$ with PBu_3, procedure B utilizes $Ni(COD)_2$ with IMes, and procedure C utilizes $Ni(COD)_2$ with IMes with syringe drive addition of the enoate, alkyne, and borane over 10 min. See the supporting information for details. [b]Combined isolated yields of the products are given. [c]Isomer ratios indicate crude ratios (from ^{1}H NMR) of the major product depicted as the first product, followed by the product epimeric at the secondary hydroxyl center, then followed by regioisomers of the alkyne insertion. [d]Complete stereostructures for entries 1, 3, 6, and 8 were unambiguously determined through reduction and acetonide formation followed by nOe analysis. In other cases, the side chain stereochemistry was assigned by analogy. In all cases, the *trans* relative configuration of the cyclopentenone ring substituents was established directly on the products obtained by the catalytic cycloaddition. See supporting information for a description of structural and stereochemical determinations.

Computational Investigation of the Mechanism. To provide deeper insight into the mechanism of the transformation, quantum chemical reaction path simulations were performed. As a starting point, prior work by our group suggests formation of a 5-membered metalacycle (**3**) from enoate and alkyne would be facile,[7] which is concurrent with mechanistic proposals of related processes.[10] From this common intermediate, several different pathways were then postulated (Scheme 3).[14] In the upper two pathways, metallacycle **3** isomerizes to 7-membered metallacycle

4, which is capable of reacting with electrophiles (i.e. aldehydes).[7a] Such aldol-first mechanisms conceivably occur through an inner-sphere (Path A, black) or outer-sphere (Path B, blue) process, and carbocyclization could occur after aldol addition from species such as **5**. Alternatively, Ogoshi has shown that cyclic *C*-enolate species such as **7** can form rapidly under aprotic conditions, via ketene intermediate **6** (Path C, red).[10b] In this ketene-first mechanism, aldol addition occurs after carbocyclization.

Scheme 3. Postulated Mechanisms for Cyclization

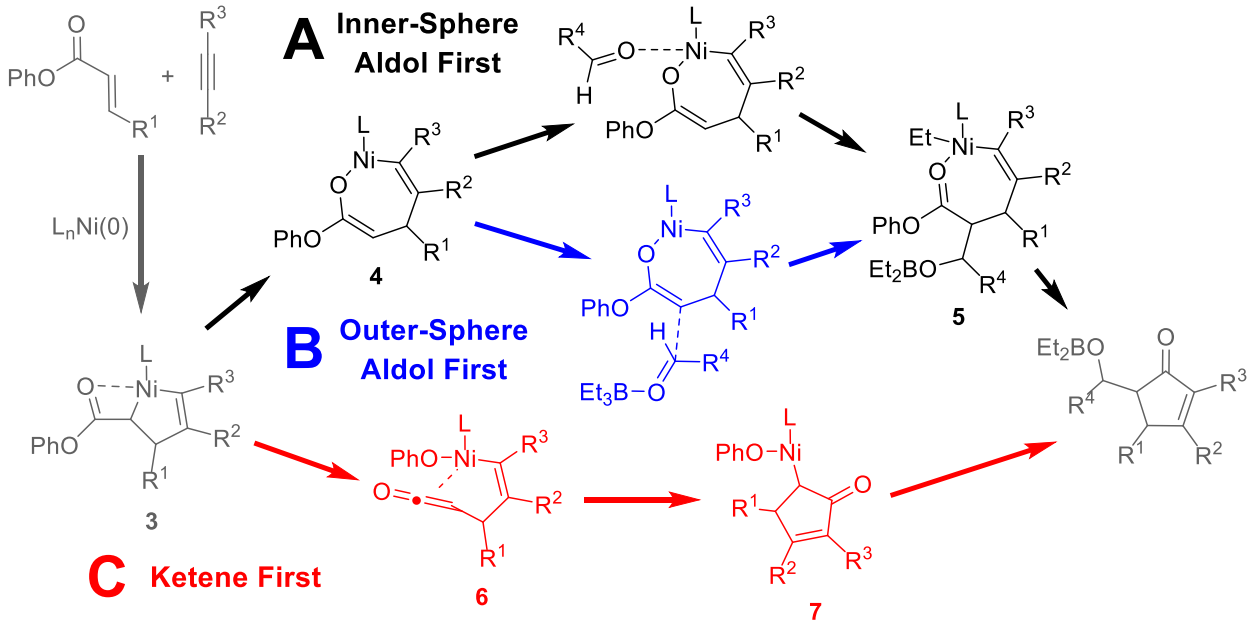

The simulation results for paths A-C are shown in Figure 1, which shows the detailed potential energy profile for the three-component cycloaddition. This reaction profile starts with complex **I**, a 5-membered metalacycle analogous to **3** of Scheme 3. **I** can isomerize to rotamer **II**, from which it can branch into the aldol-first or ketene-first pathways, respectively (Figure S1). In the aldol-first pathway, **II** isomerizes to η-3 coordinated **III-A** (Figure S1), which can subsequently rearrange to form 7-membered metallacycle **IV-A** (**TS-III-A**). The aldol-first pathways A and B split at this point. In inner-sphere path A, ligation of benzaldehyde to **IV-A**

yields complex **V-A**, which can then undergo an aldol reaction (**TS-V-A**) by a conventional 6-membered transition state. In outer-sphere path B, a triethylborane-benzaldehyde complex directly adds to metallacycle **IV-A** (**TS-IV-B**). Both aldol adducts **V-B** and **VI-A**, can then subsequently undergo carbocyclization (Figure S2). In the ketene-first pathway, extrusion of the phenoxide from **II** (**TS-II-C**) yields ketene complex **III-C**. Carbocylization of **III-C** to yield C-enolate **IV-C** is rapid and irreversible. Subsequently, benzaldehyde can coordinate to this complex, to ultimately undergo an aldol reaction (Figure S3). Phenoxide extrusion (**TS-II-C)** is thus the rate-limiting step in the ketene-first path. As this transition state is 1.4 kcal/mol lower in energy than **TS-III-A**, we predict that ketene-first pathway C is the major reaction pathway that occurs in solution.

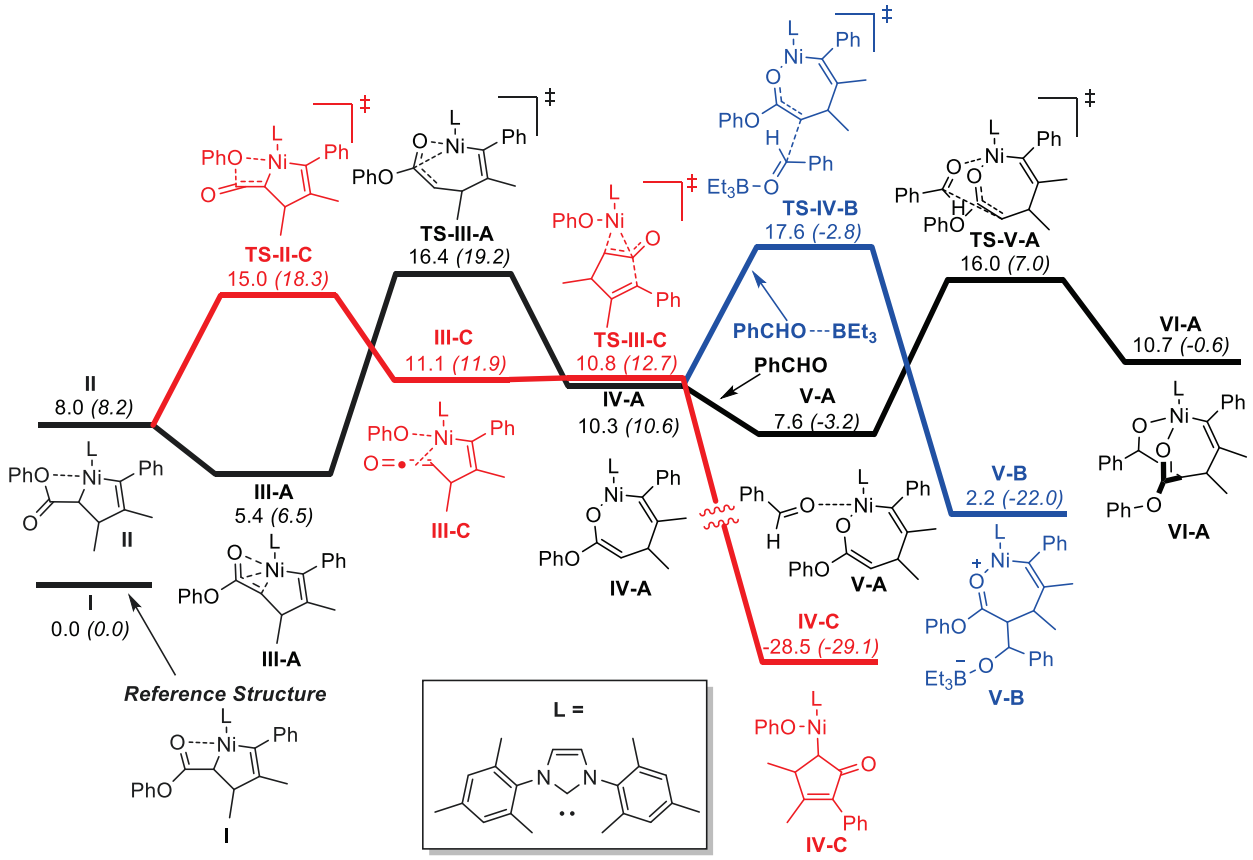

Figure 1. Comparison of Ketene-First and Aldol-First Mechanisms. Path A (black): inner-sphere

aldol-first mechanism; Path B (blue): outer-sphere aldol-first mechanism; Path C (red): ketene-first mechanism. The key ground states and transition states that influence relative rates and selectivities are depicted. Other structures on the pathways are omitted for clarity, and the complete pathways with all relevant structures are available in the supporting information (Figures S1,S2,S3). Free energies and enthalpies from ωB97X-D3/cc-pVTZ/Toluene are listed in kcal/mol, and enthalpy values are listed in italics.

Evidence of Metallacycle Formation with α-Substituted Enoates.

Considering the similarity of transition state energies of the competing pathways (**TS-II-C**, **TS-III-A**, and **TS-IV-B**), an aldol-first pathway is inherently plausible, and a minor perturbation from the system studied in Scheme 4 can push the reaction to use a different path. For instance, in the case of α-substituted enoates (and only in the case of α-substitution), small amounts of linear products can be isolated in addition to the desired carbocycle. To better understand this outcome, the coupling of PhCDO, phenyl methacrylate, and phenyl propyne led to the production of products **10** (46 %, >97% D) and **12** (23 %, >97% D) (Scheme 4). The formation of product **12**, which maintains the phenyl ester functionality, is best explained by a pathway involving the aldol addition of **8** to produce **9**, followed by β-hydride elimination to form **11**, and reductive elimination to form **12**. This redox neutral pathway was previously described in the absence of Et_3B,[15] but as this example demonstrates, the phenyl ester may be maintained under conditions optimized for the reductive cycloaddition with Et_3B. The formation of species such as **12** implies that in the α-substituted system, ketene formation does not fully outcompete isomerization to a 7-membered metallacycle and that an inner-sphere or outer-sphere aldol-first process is involved in the production of intermediate **9** in the production of **12**. The pathway leading to **10**, however, is not clarified by this result and may involve an aldol-first or ketene first mechanism.

Scheme 4. Linear Product Formation with α-Substituted Enoates

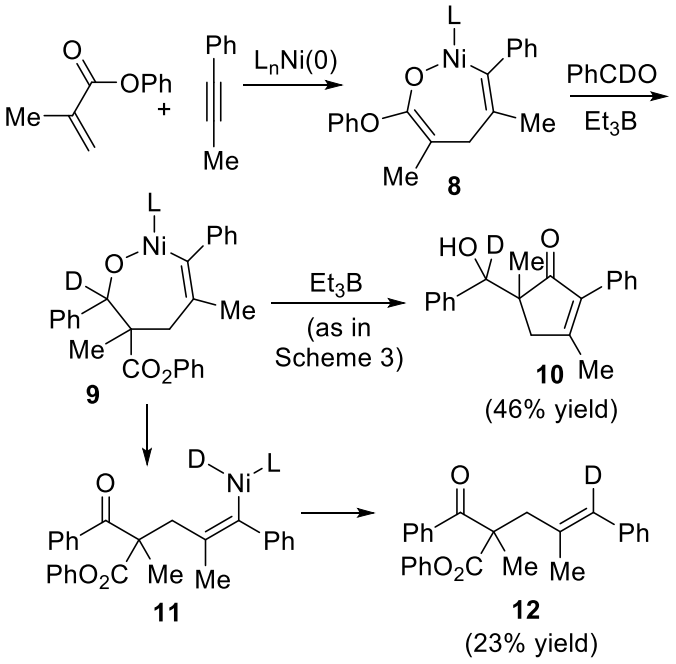

Computational analysis of the first steps with an α-substituted enoate support this explanation (Figure 2). With the inclusion of additional steric bulk near the ester, phenoxide extrusion becomes more difficult by 2.8 kcal/mol (**α-TS-II-C** vs **TS-II-C**). Isomerization to the 7-membered metallacycle is also more challenging in the α-substituted system, but only by 0.8 kcal/mol (**α-TS-III-A** vs **TS-III-A**). In this system, metallacycle formation now is predicted to outcompete ketene formation by 0.6 kcal/mol (**α-TS-II-C** vs **α-TS-II-C**), and is now the major reaction path. The relative abundance of 7-membered metalacyclic intermediates such as **α-IV-A** explains why linear products such as **12** are observed in reactions involving α-substituted enoates, but not with their β-substituted counterparts.

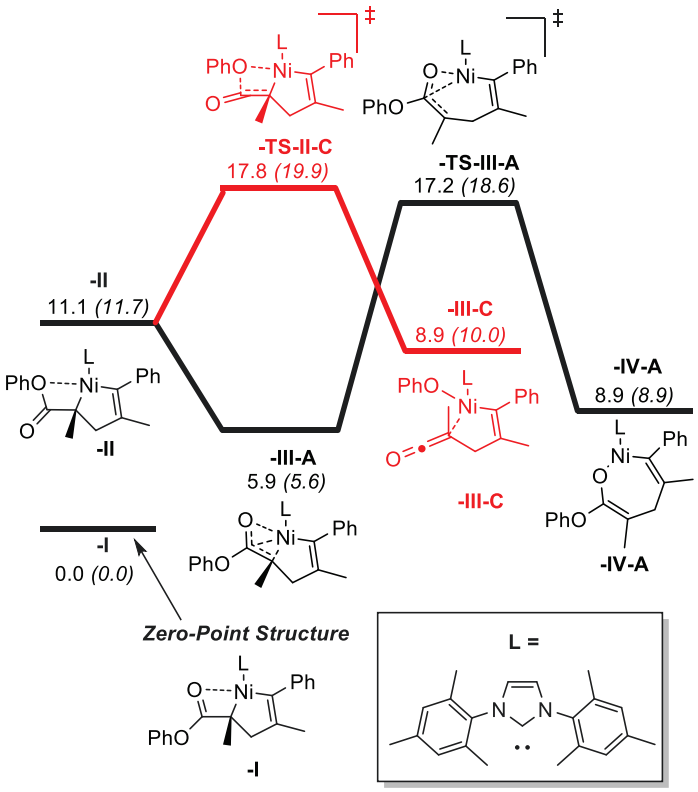

Figure 2. Ketene Formation is Disfavored with α-Substituted Enoates. Path A (black): formation of the 7-membered metallacycle; Path C (red): formation of the ketene complex. The key ground states and transition states that influence relative rates and selectivities are depicted. Other structures on the pathways are omitted for clarity, and the complete pathways with all relevant structures are available in the supporting information (Figure S4). Free energies and enthalpies ωB97X-D3/cc-pVTZ/Toluene in kcal/mol, with enthalpy values in italics.

Conclusion

In summary, a cascade reaction allowing the reductive combination of enoates, alkynes, and aldehydes to provide access to highly functionalized cyclopentenone products has been described. The sequence allows the formal [3+2] cycloaddition of the phenyl enoate and alkyne accompanied by alkylation of the enoate α-carbon with an aldehyde. Nickel catalysts supported by either phosphines or *N*-heterocyclic carbenes promote the transformation. Computational and

experimental results suggest that the ketene-first pathway is preferred, and insights into switching the selectivity from a ketene-first path to an aldol-first path have been provided. The detailed computational analysis demonstrates the precarious balance that exists between different possible addition pathways involving nickel ester enolates. A ketene-first pathway is dominant in most cases, based on the preference for phenoxide extrusion to proceed faster than intermolecular aldol addition. This selectivity can be reversed (favoring aldol addition first) when an α-substituted enoate is used, since isomerization to a 7-membered metallacycle is computationally predicted to proceed extrusion of phenoxide to form a ketene complex. The ability of this process to build considerable complexity from three simple and widely available starting materials suggests that the design principles and the understanding of the competing pathways available to nickel enoates may find use in other catalytic sequences.

Experimental Section

General Information. All reagents were used as received unless otherwise noted. Solvents were purified under nitrogen using a solvent purification system (Innovative Technology, Inc. Model # SPS-400-3 and PS-400-3. Enoates were distilled prior to use. $Ni(COD)_2$ (Strem Chemicals, Inc., used as received), 1,3-Bis(2,4,6-trimethyl-phenyl)imidazolium chloride (IMes·HCl), and potassium *tert*-butoxide were stored and weighed in an inert atmosphere glovebox. Tri-N-butylphosphine was freshly distilled and used under an inert atmosphere. Aldehydes were freshly distilled using a Buchi GKR-51 Kuegelrhor. All reactions were conducted in flame-dried or oven dried (120 °C) glassware under nitrogen atmosphere. ^{1}H and ^{13}C spectra were obtained in $CDCl_3$ at rt (25 °C), unless otherwise noted. Chemical shifts of ^{1}H NMR spectra were recorded in parts per million (ppm) on the δ scale from an internal standard of residual chloroform (7.26 ppm). Chemical shifts of ^{13}C NMR spectra were recorded in ppm from the central peak of $CDCl_3$ (77.0

ppm) on the δ scale. HPLC purification was conducted using either a Shimadzu LC-8A HPLC with a Grace PN 81116 Alltima Silica 5μm 250 x 10mm prep column or a Waters Delta 600 Agilent Zorbax RX-SIL Prep HT 21.2 x 250 mm 7μm column.

General Procedure A:

$Ni(COD)_2$ (8 mg, 0.03mmol, 0.1 equiv) was added to a vial in a glovebox and the vial was then fitted with a rubber septum, removed from the glovebox and attached to a nitrogen-filled Schlenk line. Toluene (1.5 mL) was then added to the vial and the catalyst was allowed to stir for a few min before tri-*n*-butylphosphine (15 μL, 0.06 mmol, 0.2 equiv) was added dropwise turning the pale yellow catalyst solution to bright yellow. Next, enoate (0.3 mmol, 1 equiv) was weighed out into a separate vial and the vial was placed under a nitrogen atmosphere and purged three times with nitrogen. Alkyne (0.45 mmol 1.5 equiv) and aldehyde (0.45 mmol, 1.5 equiv) were then added to the substrate vial via syringe and the vial was purged with nitrogen twice more. Toluene (0.5 mL) was added to the combined substrates and this solution was transferred by cannula to the catalyst solution washing twice with toluene (0.5 mL), resulting in a red reaction mixture. Triethylborane (217 μL, 1.5 mmol, 5 equiv) was then added immediately to the reaction via syringe, and the reaction was placed in a preheated 90 °C oil bath and stirred for 2 h before quenching with 1.5 mL saturated NH_4Cl.

General Procedure B:

$Ni(COD)_2$ (8 mg, 0.03mmol, 0.1 equiv), IMes·HCl (10 mg, 0.03 mmol, 0.1 equiv), and *t*-BuOK (3 mg, 0.03 mmol, 0.1 equiv) were added sequentially to a flame-dried vial in a glovebox. The vial was then fitted with a rubber septum, removed from the glovebox, and attached to a nitrogen-filled

Schlenk line. Toluene (1.5 mL) was then added to the catalyst, resulting in a black-yellow or brown solution after 10 min of stirring. The rest of the procedure is identical to procedure A.

General Procedure C:

$Ni(COD)_2$ (8 mg, 0.03mmol, 0.1 equiv), IMes·HCl (10 mg, 0.03 mmol, 0.1 equiv), and *t*-BuOK (3 mg, 0.03 mmol, 0.1 equiv) were added sequentially to a flame dried vial in a glovebox. The vial was then fitted with a rubber septum, removed from the glovebox and attached to a nitrogen-filled Schlenk line. Toluene (2.0 mL) was then added to the catalyst, resulting in a black-yellow or brown solution after 10 min of stirring. Next, enoate (0.3 mmol, 1 equiv) was weighed out into a separate vial, and the vial was placed under a nitrogen atmosphere and purged three times with nitrogen. Alkyne (0.45 mmol 1.5 equiv) was then added to the substrate vial and the vial was purged twice more with nitrogen. Toluene (0.5 mL) was added to the substrate vial followed by addition of triethylborane (217µL, 1.5 mmol, 5 equiv) by syringe. The substrate and reducing agent solution was drawn up into a syringe and the vial was washed with toluene twice (0.25 mL) resulting in a substrate solution volume of 1.0 mL. Aldehyde (0.45 mmol, 1.5 equiv) was then added via syringe to the stirred catalyst solution and the vial was placed in a pre-heated 90 °C oil bath followed by a 10 min addition of the 1 mL solution of substrates and reducing agent with a syringe drive. The reaction was stirred for 2 h before quenching with 1.5 mL of saturated NH_4Cl.

General Workup Procedure:

The reaction is quenched with 1.5 saturated NH_4Cl and then washed into a separatory funnel. The organic and aqueous layers are then separated and the aqueous layer is extracted twice with methylene chloride (2 mL). The organic layers were then combined and washed with 10 mL of 0.5

M NaOH followed by brine (10 mL). The organic layers are then dried with Na_2SO_4 and filtered through a pad of silica washing with 50/50 EtOAc/Hex. The solution was then concentrated to yield the crude isolate. Product ratios reported in Table 2 of the manuscript and within each experimental below were determined on crude reaction mixtures by ^1H NMR analysis.

Relative Stereochemistry Determinations:

The purified diastereomer (1 equiv) and $CeCl_3$ (1 equiv) were dissolved in 1 mL MeOH. This solution was cooled to 0 °C and $NaBH_4$ (4.5 equiv) was added in portions. The reaction was stirred until completion of the reaction was confirmed by TLC. The reaction was quenched with 1 mL NH_4Cl and extracted 3x with EtOAc. The organic layers were washed with brine and dried over Na_2SO_4. Flash chromatography of the crude isolate separated the product diastereomers.

Each diastereomer was dissolved in 1 mL DMP (dimethoxypropane) and a 1 mol % PTSA was added as a 1 mg/ 100 µL solution. After 30 min, the reaction was quenched with 1 mL sat. $NaHCO_3$ and extracted 3x with EtOAc. The organic layers were washed with brine and dried over Na_2SO_4. The crude product was purified by flash chromatography yield. Only one diastereomer will yield the desired acetonide. The other diastereomer will initially yield a ketal product, but this product is unstable and will rapidly decompose. nOe experiments are then performed on the acetonide product to determine the relative stereochemistry.

5-(Hydroxy(phenyl)methyl)-3,4-dimethyl-2-phenylcyclopent-2-enone (Table 1 and Table 2, entries 1 and 2, compounds **1a,b**)

General Procedure A was followed using phenyl 3-butenoate (49 mg, 0.3 mmol, 1 equiv) and 1-phenyl-1-propyne (56 µL, 0.45 mmol, 1.5 equiv), and benzaldehyde (46 µL, 0.45 mmol, 1.5

equiv). The reaction was then worked up using the general workup procedure, and NMR analysis of the crude isolate revealed the product in an isomeric ratio of 69:26:5. Column chromatography (5 to 20% EtOAc/Hex) yielded the products whose NMR data matched that previously published (50 mg combined, 57%).[9]

General Procedure B was followed using phenyl 3-butenoate (49 mg, 0.3 mmol, 1 equiv) and 1-phenyl-1-propyne (56 μL, 0.45 mmol, 1.5 equiv), and benzaldehyde (46 μL, 0.45 mmol, 1.5 equiv). The reaction was then worked up using the general workup procedure and NMR of the crude isolate revealed the product in an isomeric ratio of 45:35:20. Column chromatography (5 to 20% EtOAc/Hex) yielded the products whose NMR matched that previously published (54 mg combined, 61%).[10a]

trans-5-Hydroxy(phenyl)methyl)-3-methyl-2-phenylcyclopent-2-enone (Major Diastereomer, Scheme 2 and Table 2, entry 3 , compound **2a**)

General Procedure C was followed using phenyl acrylate (44 mg, 0.3 mmol, 1 equiv), 1-phenyl-1-propyne (56 μL, 0.45 mmol, 1.5 equiv), and benzaldehyde (46 μL, 0.45 mmol, 1.5 equiv). The reaction was then worked up using the general workup procedure and purified by column chromatography (10 to 30% EtOAc/Hex) to yield an impure mixture of isomers (69:25:6). Purification of the products on the Shimadzu HPLC yielded the products as a mixture of diastereomers (84:16) (40 mg, 48%). The diastereomers could be separated after additional HPLC runs revealing the major diastereomer as a white solid and the minor as an oil. ^{1}H NMR (700 MHz, $CDCl_3$): δ 7.28-7.42 (m, 10H), 5.47 (t, J = 3.9 Hz, 1H), 2.94 (m, 1H), 2.73 (d, J = 18.2 Hz, 1H), 2.58 (d, J = 4.9 Hz, 1H), 2.45 (dd, J = 18.9 Hz, J = 7.4 Hz, 1H), 2.14 (s, 3H). ^{13}C{^{1}H} NMR (176 MHz, $CDCl_3$): δ 207.8, 172.8, 142.4, 140.2, 131.5, 129.1, 128.4, 128.2, 127.7, 127.4, 125.6, 71.9,

52.8, 33.0, 18.4. IR (thin film) v: 3441, 3056, 2907, 1695, 1635, 1597, 1494, 1448, 1380, 1346, 1209, 1135, 1006, 964, 912, 762, 744, 701, 668, 586 cm^{-1}. HRMS (ESI-TOF) (m/z): $[M+H]^+$ Calc for $C_{19}H_{19}O_2$, 279.1380; found, 279.1377. nOe relationships of the dimethylketal derived from reduction of this compound were determined according to the general procedure.

cis-5-Hydroxy(phenyl)methyl)-3-methyl-2-phenylcyclopent-2-enone (Minor Diastereomer, Scheme 2 and Table 2, entry 3 , compound **2b**)

^1H NMR (700 MHz, $CDCl_3$): δ 7.30-7.45 (m, 10H), 4.98 (s, 1H), 4.74 (d, 9.8 Hz, 1H), 2.91 (ddd, J = 9.8 Hz, 7.0 Hz, 2.8 Hz), 2.49 (dd, J = 19.3 Hz, J = 7.3 Hz, 1H), 2.26 (d, J = 18.9 Hz, 1H), 2.14 (s, 3H). $^{13}C\{^1H\}$ NMR (176 MHz, $CDCl_3$): δ 210.3, 172.7, 141.5, 139.5, 130.1, 129.1, 128.6, 128.4, 128.2, 128.0, 75.7, 51.3, 35.7, 18.3. IR (thin film) v: 3442, 1676, 1635, 1494, 1429, 1381, 1346, 1205, 1140, 1040, 911, 737, 701 cm^{-1}. HRMS (ESI-TOF) (m/z): $[M+Na]^+$ Calc for $C_{19}H_{18}O_2Na$, 301.1199; found, 301.1199.

5-(Hydroxy(phenyl)methyl)-3,5-dimethyl-2-phenylcyclopent-2-enone (Major Diastereomer, Table 2, entries 4 and 5)

General Procedure A was followed using phenyl methacrylate (49 mg, 0.3 mmol, 1.0 equiv), 1-phenyl-1-propyne (56 μL, 0.45 mmol, 1.5 equiv), and benzaldehyde (46 μL, 0.45 mmol, 1.5 equiv). The reaction was worked up using the general workup procedure and the NMR revealed the isomeric ratio of the crude to be (61:39). This crude isolate was then subjected to column chromatography (10 to 20% EtOAc/Hex) and 48 mg combined (54 %) of product was isolated. The diastereomers could be separated with additional flash chromatography revealing the major diastereomer as a white solid and the minor as a colorless oil. ^1H NMR (700 MHz, $CDCl_3$): δ 7.28-

7.42 (m, 10H), 4.97 (d, J = 4.9 Hz, 1H), 3.12 (d, J = 18.2 Hz, 1H), 2.70 (d, J = 4.2 Hz, 1H), 2.13 (s, 3H), 2.10 (d, J = 18.2 Hz, 1H), 1.15 (s, 3H). $^{13}C\{^{1}H\}$ NMR (176 MHz, $CDCl_3$): δ 211.3, 171.2, 141.0, 138.5, 131.7, 129.1, 128.2, 128.1, 127.8, 127.6, 127.2, 76.8, 52.3, 41.7, 22.9, 18.3. IR (thin film) v: 3443, 2928, 1689, 1639, 1495, 1380, 1044, 909, 744, 700 cm^{-1}. HRMS (ESI-TOF) (m/z): $[M+H]^+$ Calc for $C_{20}H_{21}O_2$, 293.1536; found, 293.1533.

General Procedure B was followed using phenyl methacrylate (49 mg, 0.3 mmol, 1.0 equiv), 1-phenyl-1-propyne (56 μL, 0.45 mmol, 1.5 equiv), and benzaldehyde (46 μL, 0.45 mmol, 1.5 equiv). The reaction was then worked up using the general workup procedure and NMR spectroscopy revealed a 46:36:12:6 distribution of isomers. Column chromatography (10 to 20%) of the crude concentrate yielded the product as an oil in a 52:36:11 ratio (44 mg, 50%).

5-(Hydroxy(phenyl)methyl)-3,5-dimethyl-2-phenylcyclopent-2-enone (Minor Diastereomer, Table 2, Entries 4 and 5)

^{1}H NMR (700 MHz, $CDCl_3$): δ 7.38-7.40 (m, 4H), 7.26-7.34 (m, 4H), 7.18 (d, J = 7.7 Hz, 2H), 4.85 (s, 1H), 3.95 (s, 1H), 2.86 (d, J = 19.6 Hz, 1H), 2.15 (d, J = 18.9 Hz, 1H), 2.08 (s, 3H), 1.32 (s, 3H). $^{13}C\{^{1}H\}$ NMR (176 MHz, $CDCl_3$): δ 212.4, 171.0, 140.0, 138.0, 131.3, 129.0, 128.2, 127.9, 127.8, 127.7, 127.3, 76.7, 51.2, 43.3, 18.9, 18.1. IR (thin film) v: 3443, 2929, 1688, 1638, 1495, 1452, 1381, 1046, 739, 700 cm^{-1}. HRMS (ESI-TOF) (m/z): $[M+H]^+$ Calc for $C_{20}H_{21}O_2$, 293.1536; found, 293.1532.

5-(Hydroxy(phenyl)methyl)-3-methyl-2,4-diphenylcyclopent-2-enone (Major Diastereomer, Table 2, Entry 6)

General Procedure C was followed using phenyl cinnamate (67 mg, 0.3 mmol, 1 equiv), 1-phenyl-1-propyne (56 μL, 0.45 mmol, 1.5 equiv), and benzaldehyde (46 μL, 0.45 mmol, 1.5 equiv). The reaction was then worked up using the general workup procedure and purified by column chromatography (10 to 20% EtOAc/Hex) to yield an impure mixture of isomers (65:29:6). Further column chromatography and HPLC purification on the Waters HPLC yielded the major diastereomer as a white solid (28 mg) and the minor diastereomer as a colorless oil (10 mg) and mixture of isomers (15 mg, 50:29:15:6) (53 mg, 50%). ^{1}H NMR (700 MHz, $CDCl_3$): δ 7.44 (t, J = 7.4 Hz, 2H), 7.34-7.39 (m, 5H), 7.28 (t, J = 7.7 Hz, 2H), 7.23 (t, J = 7.7 Hz, 1H), 7.12-7.13 (m, 3H), 6.70-6.72 (m, 2H), 5.51 (t, J = 4.2 Hz, 1H), 3.88 (d, J = 2.1 Hz, 1H), 2.92 (t, J = 3.2 Hz, 1H), 2.68 (d, 4.9 Hz, 1H), 1.91 (s, 3H). ^{13}C{^{1}H} NMR (176 MHz, $CDCl_3$): δ 207.4, 174.4, 141.6, 141.2, 141.1, 131.4, 129.2, 128.6, 128.3, 128.2, 127.9, 127.4, 127.3, 126.7, 125.6, 72.2, 62.5, 50.3, 16.8. IR (thin film) v: 3445, 3026, 1682, 1630, 1495, 1379, 1149, 1054, 908, 763, 728, 698, 602, 574 cm^{-1}. HRMS (ESI-TOF) (m/z): $[M+H]^+$ Calc for $C_{25}H_{23}O_2$, 355.1693; found, 355.1693. nOe relationships of the acetonide derived from reduction of this compound were determined according to the general procedure above.

5-(Hydroxy(phenyl)methyl)-3-methyl-2,4-diphenylcyclopent-2-enone (Minor Diastereomer, Table 2, Entry 6)

^{1}H NMR (700 MHz, $CDCl_3$): δ 7.45-7.47 (m, 2H), 7.38-7.39 (m, 3H), 7.26-7.30 (m, 5H), 7.10-7.13 (m, 3H), 6.52 (d, J = 7.0 Hz, 2H), 4.82 (d, J = 9.8 Hz, 1H), 4.75 (s, 1H), 3.45 (s, 1H), 2.85 (dd, J = 9.8 Hz, J = 2.8 Hz, 1H), 1.91 (s, 3H). ^{13}C{^{1}H} NMR (176 MHz, $CDCl_3$): δ 209.7, 174.5, 140.7, 140.2, 140.1, 130.8, 129.2, 128.7, 128.5, 128.4, 128.3, 128.2, 127.4, 127.3, 126.9, 75.9, 61.4, 52.7, 16.9. IR (thin film) v: 3449, 3028, 2916, 1679, 1635, 1599, 1494, 1454, 1377, 1334,

1203, 1146, 1039, 912, 761, 735, 699, 572 cm^{-1}. HRMS (ESI-TOF) (m/z): $[M+H]^+$ calc for $C_{25}H_{23}O_2$, 355.1693; found, 355.1693.

trans-5-(Hydroxy(phenyl)methyl)-4-methyl-2,3-dipropylcyclopent-2-enone (Major Diastereomer, Table 2, Entry 7)

General Procedure B was followed using phenyl 3-butenoate (49 mg, 0.3 mmol, 1 equiv) and 4-octyne (66 µL, 0.45 mmol, 1.5 equiv), and benzaldehyde (46 µL, 0.45 mmol, 1.5 equiv). The reaction was then worked up using the general workup procedure and NMR revealed two diastereomers (58:42). The crude reaction mixture was subjected to column chromatography (10 to 20% EtOAc/Hex) to yield an impure and unseparated diastereomers. Further column chromatography (0.5% MeOH/CH_2Cl_2) resulted in purification and partial separation of the product diastereomers yielding 14 mg of the minor diastereomer, 16 mg of the major diastereomer, and 15 mg of both diastereomers (58:42) all as colorless oils (44 mg combined, 52%). ^1H NMR (700 MHz, $CDCl_3$): δ 7.32-7.33 (m, 4H), 7.25-7.26 (m, 1H), 5.33 (t, J = 4.2 Hz, 1H), 2.83 (d, J = 5.6 Hz, 1H), 2.75 (q, J = 7.0 Hz, 1H), 2.40 (ddd, J = 14.0 Hz, 9.1 Hz, 7.7 Hz, 1H), 2.31 (t, J = 2.8 Hz, 1H), 2.23 (ddd, J = 14.0 Hz, 9.1 Hz, 4.9 Hz, 1H), 2.08-2.16 (m, 2H), 1.48-1.56 (m, 1H), 1.39 (sext, J = 7.7 Hz, 2H), 1.28-1.36 (m, 1H), 0.86 (t, J = 5.6 Hz, 3H), 0.86 (t, J = 6.0 Hz, 3H), 0.80 (d, J = 7.0 Hz, 3H). $^{13}C\{^1H\}$ NMR (176 MHz, $CDCl_3$): δ 209.6, 178.8, 142.1, 140.0, 128.2, 127.3, 125.6, 72.3, 60.0, 35.8, 30.3, 25.1, 21.8, 20.7, 18.1, 14.1, 14.0. IR (thin film) v: 3402, 2959, 1684, 1635, 1450, 1372, 1084, 701, 556 cm^{-1}. HRMS (ESI-TOF) (m/z): $[M+H]^+$ Calc for $C_{19}H_{27}O_2$, 287.2006; found, 287.2007.

5-(Hydroxy(phenyl)methyl)-4-methyl-2,3-dipropylcyclopent-2-enone (Minor Diastereomer, Table 2, Entry 7)

^{1}H NMR (700 MHz, $CDCl_3$): δ 7.29-7.39 (m, 5H), 5.09 (s, 1H), 4.57 (d, J = 9.8 Hz, 1H), 2.43 (ddd, 14.0 Hz, 9.1 Hz, 7.0 Hz, 1H), 2.32 (q, J = 7.0 Hz, 1H), 2.23 (ddd, J = 14.0 Hz, 9.1 Hz, 4.9 Hz, 1H) 2.11-2.20 (m, 3H), 1.52-1.57 (m, 1H), 1.42 (quind, J = 7.0 Hz, 3.5Hz, 2H), 1.36-1.39 (m, 1H), 0.93 (t, J = 7.7 Hz, 3H), 0.90 (t, J = 7.7 Hz, 3H), 0.63 (d, J = 7.0 Hz, 3H). ^{13}C{^{1}H} NMR (176 MHz, $CDCl_3$): δ 211.7, 178.8, 141.6, 139.2, 128.4, 128.1, 126.9, 75.9, 59.1, 38.4, 30.3, 25.0, 21.8, 20.8, 17.5, 14.2, 14.0. IR (thin film) v: 3436, 2961, 2872, 1676, 1630, 1454, 1383, 1048, 703 cm^{-1}. HRMS (ESI-TOF) (m/z): $[M+H]^+$ Calc for $C_{19}H_{27}O_2$, 287.2006; found, 287.2007.

5-(1-Hydroxy-2-methylpropyl)-3,4-dimethyl-2-phenylcyclopent-2-enone (Major Diastereomer, Table 2, Entry 8)

General Procedure A was followed using phenyl 3-butenoate (49 mg, 0.3 mmol, 1 equiv) and 1-phenyl-1-propyne (56 µL, 0.45 mmol, 1.5 equiv), and isobutyraldehyde (41 µL, 0.45 mmol, 1.5 equiv). Procedural Note: This reaction was conducted in a sealed tube instead of a vial. The reaction was worked up using the general workup procedure and NMR of the crude reaction revealed a (37:63) ratio of isomers. The crude isolate was subjected to column chromatography (5 to 20% EtOAc/Hex) followed by purification on a Waters HPLC (97:3 Hex/(20% *i*-PrOH/Hex) yielding 18 mg of the major diastereomer as a colorless oil and 22 mg of the minor diastereomer as a white solid (40 mg combined, 52%). ^{1}H NMR (700 MHz, $CDCl_3$): δ 7.41 (t, J = 7.7 Hz, 2H), 7.33 (t, J = 6.3 Hz, 1H), 7.28 (d, J = 7.7 Hz, 2H), 4.39 (s, 1H), 3.58 (d, J = 9.1 Hz, 1H), 2.53 (q, J = 6.5 Hz, 1H), 2.22 (d, J = 9.8 Hz, 1H), 2.15 (s, 3H), 1.86 (quint, J = 6.3 Hz, 1H), 1.33 (d, J = 7.0 Hz, 3H), 1.10 (d, J = 7.0 Hz, 3H), 1.02 (d, J = 7.0 Hz, 3H). ^{13}C{^{1}H} NMR (176 MHz, $CDCl_3$): δ

210.5, 176.0, 139.2, 131.2, 129.1, 128.3, 127.8, 76.6, 55.4, 41.5, 31.4, 20.4, 18.0, 15.9, 14.9. IR (thin film) v: 3455, 2963, 1675, 1635, 1598, 1493, 1419, 1380, 1342, 1270, 1154, 1003, 733, 699 cm^{-1}. HRMS (ESI-TOF) (m/z): $[M+H]^+$ Calc for $C_{17}H_{23}O_2$, 259.1693; found, 259.1694.

5-(1-Hydroxy-2-methylpropyl)-3,4-dimethyl-2-phenylcyclopent-2-enone (Minor Diastereomer, Table 2, Entry 8)

^1H NMR (700 MHz, $CDCl_3$): δ 7.40 (t, J = 7.7 Hz, 2H), 7.27-7.35 (m, 3H), 3.90 (ddd, J = 8.5 Hz, J = 5.5 Hz, J = 2.5 Hz, 1H), 2.95 (q, J = 5.4 Hz, 1H), 2.37 (t, J = 2.8 Hz, 1H), 2.15 (s, 3H), 1.90 (dsept, J = 2.5 Hz, J = 6.5 Hz, 1H), 1.73 (d, J = 5.0 Hz, 1H), 1.33 (d, J = 7.0 Hz, 3H), 1.10 (d, J = 7.0 Hz, 3H), 1.00 (d, J = 7.0 Hz, 3H). $^{13}C\{^1H\}$ NMR (125 MHz, $CDCl_3$): δ 208.1, 176.2, 139.9, 131.9, 129.2, 128.2, 127.6, 76.8, 56.8, 38.5, 31.8, 19.7, 19.1, 18.6, 15.9. IR (thin film) v: 3439, 2961, 1685, 1635, 1598, 1444, 1379, 1341, 1152, 1079, 997, 751, 700 cm^{-1}. HRMS (ESI-TOF) (m/z): $[M+H]^+$ Calc for $C_{17}H_{23}O_2$, 259.1693; found, 259.1698. nOe relationships of the acetonide derived from reduction of this compound were established according to the general procedure above.

trans-3-(3-((*tert*-Butyldimethylsilyl)oxy)propyl)-5-(hydroxy(phenyl)methyl)-4-methyl-2-phenylcyclopent-2-enone (Major Diastereomer, Table 2, Entry 9)

General Procedure B was followed using phenyl 3-butenoate (49 mg, 0.3 mmol, 1 equiv) and tert-butyldimethyl((5-phenylpent-4-yn-1-yl)oxy)silane (123 mg, 0.45 mmol, 1.5 equiv), and benzaldehyde (46 μL, 0.45 mmol, 1.5 equiv). The reaction was worked up using the general workup procedure and subjected to column chromatography yielding a crude mixture of isomers (54:37:9). These isomers were able to be further purified and separated using the Shimadzu HPLC

yielding 19 mg of pure minor diastereomer as a colorless oil, 44 mg of pure major diastereomer as a white solid, and an additional 14 mg of mixed isomers (22:68:10) as a colorless oil (77 mg, 57%). ^{1}H NMR (700 MHz, $CDCl_3$): δ 7.35-7.41 (m, 6H), 7.31 (t, J = 7.0 Hz, 1H), 7.28 (t, J = 7.0 Hz, 1H), 7.22 (d, J = 6.8 Hz, 2H), 5.44 (d, J = 1.4 Hz, 1H), 3.56 (dt, J = 10.5 Hz, 5.6 Hz, 1H), 3.47 (ddd, J = 10.5 Hz, 7.0 Hz, 5.6 Hz, 1H), 2.96 (qd, J = 7.0 Hz, 2.8 Hz, 1H), 2.75 (s, 1H), 2.68 (ddd, J = 7.0 Hz, 10.5 Hz, 5.6 Hz, 1H), 2.49 (t, J = 2.8 Hz, 1H), 2.37 (ddd, J = 13.3 Hz, 10.0 Hz, 4.4 Hz, 1H), 1.69 (dtt, J = 16.1 Hz, 7.7 Hz, 5.6 Hz, 1H), 1.50 (dquin, J = 18.2 Hz, 5.6 Hz, 1H), 0.89 (d, J = 7.7 Hz, 3H), 0.84 (s, 9H), -0.01 (s, 3H), -0.02 (s, 3H). ^{13}C{^{1}H} NMR (176 MHz, $CDCl_3$): δ 207.4, 180.1, 142.0, 140.1, 131.7, 129.1, 128.3, 128.2, 127.7, 127.4, 125.6, 72.2, 62.3, 60.6, 35.9, 30.6, 25.8, 25.3, 18.2, 17.9, -5.4, -5.5. IR (thin film) v: 3446, 2955, 2856, 1684, 1630, 1597, 1495, 1471, 1360, 1255, 1152, 1099, 959, 835, 776, 702 cm^{-1}. HRMS (ESI-TOF) (m/z): $[M+H]^+$ Calc for $C_{28}H_{39}O_3Si$, 451.2663; found, 451.2672.

trans-3-(3-((*tert*-Butyldimethylsilyl)oxy)propyl)-5-(hydroxy(phenyl)methyl)-4-methyl-2-phenylcyclopent-2-enone (Minor Diastereomer, Table 2, Entry 9)

^{1}H NMR (700 MHz, $CDCl_3$): δ 7.38-7.44 (m, 6H), 7.33-7.35 (m, 2H), 7.25 (d, J = 7.0 Hz, 2H), 5.01 (s, 1H), 4.74 (d, J = 9.8 Hz, 1H), 3.57 (dt, J = 5.6 Hz, 10.5 Hz, 1H), 3.52 (ddd, J = 9.8 Hz, 7.0 Hz, 5.6 Hz, 1H), 2.71 (ddd, J = 13.3 Hz, 10.5 Hz, 5.6 Hz, 1H), 2.53 (qd, J = 7.0 Hz, 4.2 Hz, 1H), 2.36-2.41 (m, 2H), 1.70 (dtt, J = 16.8 Hz, 7.7 Hz, 5.6 Hz, 1H), 1.50-1.56 (m, 1H), 0.84 (s, 9H), 0.75 (d, J = 7.0 Hz, 3H), -0.01 (s, 3H), -0.01 (s, 3H). ^{13}C{^{1}H} NMR (176 MHz, $CDCl_3$): δ 209.0, 180.2, 141.4, 139.3, 131.1, 129.1, 128.5, 128.4, 128.2, 127.9, 126.9, 75.7, 62.4, 59.5, 38.5, 30.6, 25.8, 25.5, 18.2, 17.2, -5.4, -5.4. IR (thin film) v: 3443, 2927, 2855, 1679, 1631, 1597, 1494, 1471,

1360, 1256, 1149, 1099, 956, 834, 775, 700 cm^{-1}. HRMS (ESI-TOF) (m/z): $[M+H]^+$ Calc for $C_{28}H_{39}O_3Si$, 451.2663; found, 451.2662.

Methyl-3-*trans*-4-(hydroxy(phenyl)methyl)-5-methyl-3-oxo-2-phenylcyclopent-1-en-1-yl)propanoate (Major Diastereomer, Table 2, Entry 10)

General Procedure B was followed using phenyl 3-butenoate (49 mg, 0.3 mmol, 1 equiv) and methyl-5-phenylpent-4-ynoate (85 mg, 0.45 mmol, 1.5 equiv), and benzaldehyde (46 μL, 0.45 mmol, 1.5 equiv). The reaction was worked up using the general workup procedure and NMR spectroscopy revealed a 54:33:13 mixture of isomers. This product was further purified using column chromatography (10 to 40% EtOAc/Hex) yielding impure unseparated isomers. These isomers could be further purified and separated using the Waters HPLC (85:15 (Hex/(*i*-PrOH/Hex)) yielding 13 mg of pure major diastereomer as a white solid, 13 mg of the pure minor diastereomer, as a colorless oil, and 25 mg of mixed isomers (62:17:14:7) as a colorless oil (51 mg, 47%). ^1H NMR (500 MHz, $CDCl_3$): δ 7.27-7.43 (m 8H), 7.20-7.22 (m, 2H), 5.45 (dd, J = 5.0 Hz, J = 3.5 Hz, 1H), 3.63 (s, 3H), 2.91-2.97 (m, 2H), 2.59-2.66 (m, 2H), 2.51 (t, J = 3.0 Hz, 1H), 2.44 (ddd, J = 16.0 Hz, 10.0 Hz, 5.5 Hz, 1H), 2.32 (ddd, J = 15.5 Hz, 8.5 Hz, 7.0 Hz, 1H), 0.90 (d, J = 7.5 Hz, 3H). $^{13}C\{^1H\}$ NMR (176 MHz, CD_3CN): δ 207.0, 177.9, 173.5, 144.5, 141.4, 133.4, 130.2, 129.2, 129.1, 128.6, 127.9, 126.5, 72.2, 62.0, 52.3, 36.3, 32.1, 24.8, 18.5. IR (thin film) v: 3465, 2959, 1736, 1699, 1493, 1443, 1345, 1197, 765, 703. HRMS (ESI-TOF) (m/z): $[M+H]^+$ Calc for $C_{23}H_{25}O_4$, 365.1747; found, 365.1750.

Methyl-3-*trans*-4-(hydroxy(phenyl)methyl)-5-methyl-3-oxo-2-phenylcyclopent-1-en-1-yl)propanoate (Minor Diastereomer, Table 2, Entry 10)

^{1}H NMR (400 MHz, $CDCl_3$): δ 7.34-7.44 (m, 8H), 7.22 (d, J = 6.8 Hz, 2H), 4.83 (s, 1H), 4.75 (d, J = 9.6 Hz, 1H), 3.63 (s, 3H), 2.98 (ddd, J = 14.6 Hz, 9.1 Hz, 7.1 Hz, 1H), 2.62 (ddd, J = 14.8 Hz, 9.2 Hz, 5.6 Hz, 1H), 2.52 (qd, J = 6.8 Hz, 2.4 Hz, 1H), 2.39-2.47 (m, 2H), 2.33 (ddd, J = 16.0 Hz, 9.4 Hz, 7.0 Hz, 1H), 0.78 (d, J = 7.2 Hz, 3H). ^{13}C{^{1}H} NMR (133 MHz, $CDCl_3$): δ 209.3, 177.2, 172.2, 141.2, 140.2, 130.8, 129.0, 128.6, 128.5, 128.3, 128.2, 126.9, 75.5, 59.5, 51.9, 38.4, 31.4, 24.0, 17.5. IR (thin film) v: 3454, 2961, 1734, 1695, 1635, 1597, 1493, 1436, 1345, 1199, 1048, 913, 765, 736, 702 cm^{-1}. HRMS (ESI-TOF) (m/z): $[M+Na]^+$ Calc for $C_{23}H_{24}O_4Na$, 387.1569; found, 387.1571.

5-(1-Deutero,1-hydroxy(phenyl)methyl)-3,5-dimethyl-2-phenylcyclopent-2-enone (Major Diastereomer, Scheme 4, compound **10**)

General Procedure B was followed using phenyl methacrylate (49 mg, 0.3 mmol, 1.0 equiv), 1-phenyl-1-propyne (56 µL, 0.45 mmol, 1.5 equiv), and D-benzaldehyde (46 µL, 0.45 mmol, 1.5 equiv). The reaction was then worked up using the general workup procedure and the crude was subjected to column chromatography (10 to 20% EtOAc/Hex). Further purification on the Waters HPLC yielded the pure major diastereomer as a white solid (25 mg) and the minor diastereomer as a colorless oil (15 mg) (40 mg, 46%). ^{1}H NMR (400 MHz, $CDCl_3$): δ 7.26-7.42 (m, 10H), 3.12 (d, J = 18.4 Hz, 1H), 2.69 (s, 1H), 2.08-2.12 (m, 4H), 1.14 (s, 3H). ^{13}C{^{1}H} NMR (176 MHz, CD_3CN): δ 211.3, 172.3, 143.0, 138.7, 133.6, 130.2, 129.1, 128.8, 128.5, 128.5, 128.4, 77.0 (t, J = 22.4), 53.1, 41.7, 22.9, 18.3. IR (thin film) v: 3445, 3056, 1688, 1638, 1598, 1494, 1446, 1380, 1345, 1221, 1117, 1057, 901, 779, 743 cm^{-1}. HRMS (ESI-TOF) (m/z): $[M+H]^+$ Calc for $C_{20}H_{20}O_2D$, 294.1599; found, 294.1598.

5-(1-Deutero,1-hydroxy(phenyl)methyl)-3,5-dimethyl-2-phenylcyclopent-2-enone (Minor Diastereomer, Scheme 4, compound **10**)

^{1}H NMR (400 MHz, $CDCl_3$): δ 7.37 (t, J = 6.8 Hz, 4H), 7.27-7.34 (m, 4H), 7.16 (d, J = 7.2 Hz, 2H), 3.92 (s, 1H), 2.84 (d, J = 19.2 Hz, 1H), 2.13 (d, J = J = 19.2 Hz, 1H), 2.06 (s, 3H), 1.31 (s, 3H). ^{13}C{^{1}H} NMR (176 MHz, CD_3CN): δ 211.5, 172.6, 142.3, 139.3, 133.2, 130.0, 128.9, 128.5, 128.3, 128.3, 127.8, 77.2 (J = 22.1 Hz), 53.6, 42.3, 21.6, 17.8. IR (thin film) v: 3443, 3056, 2928, 1684, 1637, 1597, 1495, 1447, 1380, 1345, 1232, 1089, 1058, 1031, 904, 873, 776, 737, 701, 666, 546 cm^{-1}. HRMS (ESI-TOF) (m/z): $[M+H]^+$ Calc for $C_{20}H_{20}O_2D$, 294.1599; found, 294.1592.

(*E*)-5-Deutero-phenyl-2-benzoyl-2,4-dimethyl-5-phenylpent-4-enoate (Scheme 4, compound **12**) General Procedure B was followed using phenyl methacrylate (49 mg, 0.3 mmol, 1.0 equiv), 1-phenyl-1-propyne (56 µL, 0.45 mmol, 1.5 equiv), and D-benzaldehyde (46 µL, 0.45 mmol, 1.5 equiv). The reaction was then worked up using the general workup procedure and the crude was subjected to column chromatography (10 to 20% EtOAc/Hex). Further column chromatography (2.5% Acetone/Hex) of the impure isolate yielded the pure product as a white solid (26 mg, 23%). ^{1}H NMR (500 MHz, $CDCl_3$): δ 8.03 (d, J = 8.0 Hz, 2H), 7.61 (t, J = 7.5 Hz, 1H), 7.51 (t, J = 7.8 Hz, 2H), 7.33 (t, J = 7.8 Hz, 2H), 7.17-7.29 (m, 6H), 6.74 (d, J = 8.0 Hz, 2H), 3.22 (d, J = 14.0 Hz, 1H), 3.13 (d, J = 14.0 Hz, 1H), 1.89 (s, 3H), 1.80 (s, 3H). ^{13}C{^{1}H}NMR (176 MHz, $CDCl_3$): δ 197.0, 172.9, 150.3, 137.6, 135.9, 133.5, 132.9, 130.6 (t, J = 22.8 Hz) 129.4, 129.0, 128.8, 128.6, 128.1, 126.4, 126.1, 121.0, 57.5, 47.4, 21.6, 19.6. IR (thin film) v: 3057, 1753, 1684, 1597, 1492, 1446, 1378, 1304, 1192, 1089, 1024, 1001, 969, 936, 796, 748 cm^{-1}. HRMS (ESI-TOF) (m/z): $[M+H]^+$ calc for $C_{26}H_{24}O_3D$, 386.1861; found, 386.1861.

Computational Details:

Density functional calculations were performed using Q-Chem 3.1.0.0[16] for geometry optimization and frequency calculations, and ORCA 4.0.0.2[17] for single point calculations. All geometries for intermediates and transition states were optimized using the ωB97X density functional[18] and 6-31G(d) basis set.[19] Energies were refined by applying the ωB97X-D3 density functional[20] with the cc-pVTZ basis[21] and the SMD implicit solvent model[22] with toluene as the solvent ($\epsilon = 2.4$). Transition state geometries and minimum energy reaction paths were found using the single-[23] and double-ended[24] growing string methods. Found transition states were subsequently re-optimized after the initial search. All energies listed are Gibbs free energies with enthalpy and entropy corrections at 363 K. Entropy corrections were scaled to 50% to account for the difference in entropy between the gas and solvated phases.[25] The effects of low frequency oscillations were reassigned to 50 cm^{-1} to prevent the highly anharmonic vibrations from overly influencing the free energy. All intermediates and transition states were confirmed to have the appropriate number of imaginary frequencies: one for transition states, and none for intermediates. All geometry optimizations, frequency calculations, were performed with an SCF convergence tolerance of 10^{-6}. Single point calculations were performed with an SCF convergence tolerance of 10^{-8}.

Supporting Information

Stereochemical analysis, spectral data, structure cartesian coordinates (Table S1), and supplementary potential energy surfaces (Figures S1-S4). This material is available free of charge via the Internet at http://pubs.acs.org.

Acknowledgments

This work was supported by NSF grant CHE-1565837 (JM) and NIH grant R35GM128830 (PMZ). The Nagorny group is thanked for assistance with HPLC purifications.

References and Footnotes

(1) (a) Stanley, L. M.; Sibi, M. P. Enantioselective Copper-Catalyzed 1,3-Dipolar Cycloadditions. *Chem. Rev.* **2008**, *108*, 2887-2902. (b) Nair, V.; Suja, T. D. Intramolecular 1,3-dipolar cycloaddition reactions in targeted syntheses. *Tetrahedron* **2007**, *63*, 12247-12275. (c) Welker, M. E. 3 + 2 Cycloaddition reactions of transition-metal 2-alkynyl and η^1-allyl complexes and their utilization in five-membered-ring compound syntheses. *Chem. Rev.* **1992**, *92*, 97-112. (d) Trost, B. M. [3+2] Cycloaddition Approaches to Five-Membered Rings via Trimethylenemethane and Its Equivalents. *Angew. Chem. Int. Ed.* **1986**, *25*, 1-20. (e) Nakamura, I.; Yamamoto, Y. Transition Metal-Catalyzed Reactions of Methylenecyclopropanes. *Adv. Synth. Cat* **2002**, *344*, 111-129.

(2) (a) Pohlhaus, P. D.; Johnson, J. S. Enantiospecific Sn(II)- and Sn(IV)-Catalyzed Cycloadditions of Aldehydes and Donor−Acceptor Cyclopropanes. *J. Am. Chem. Soc.* **2005**, *127*, 16014-16015. (b) Lebold, T. P.; Kerr, M. A. Intramolecular annulations of donor–acceptor cyclopropanes. *Pure Appl. Chem.* **2010**, *82*, 1797-1812. (c) Reissig, H.-U.; Zimmer, R. Donor−Acceptor-Substituted Cyclopropane Derivatives and Their Application in Organic Synthesis. *Chem. Rev.* **2003**, *103*, 1151-1196. (d) Feldman, K. S.; Romanelli, A. L.; Ruckle, R. E.; Miller, R. F. Cyclopentane synthesis via free radical mediated addition of functionalized alkenes to substituted vinyl cyclopropanes. *J. Am. Chem. Soc.* **1988**, *110*, 3300-3302. (e) Qi, X.; Ready, J. M. Synthesis of Cyclopentenones from Cyclopropanes and Silyl Ynol Ethers. *Angew. Chem. Int. Ed.* **2008**, *47*, 7068-7070. (f) Liu, L.; Montgomery, J. Dimerization of Cyclopropyl

Ketones and Crossed Reactions of Cyclopropyl Ketones with Enones as an Entry to Five-Membered Rings. *J. Am. Chem. Soc.* **2006**, *128*, 5348-5349. (g) Ogoshi, S.; Nagata, M.; Kurosawa, H. Formation of Nickeladihydropyran by Oxidative Addition of Cyclopropyl Ketone. Key Intermediate in Nickel-Catalyzed Cycloaddition. *J. Am. Chem. Soc.* **2006**, *128*, 5350-5351.

(3) (a) Davies, H. M. L.; Xiang, B.; Kong, N.; Stafford, D. G. Catalytic Asymmetric Synthesis of Highly Functionalized Cyclopentenes by a [3 + 2] Cycloaddition. *J. Am. Chem. Soc.* **2001**, *123*, 7461-7462. (b) Davies, H. M. L.; Hu, B. B.; Saikali, E.; Bruzinski, P. R. Carbenoid versus Vinylogous Reactivity in Rhodium(II)-Stabilized Vinylcarbenoids. *J. Org. Chem.* **1994**, *59*, 4535-4541. (c) Barluenga, J.; Barrio, P.; Riesgo, L.; Lopez, L. A.; Tomas, M. A General and Regioselective Synthesis of Cyclopentenone Derivatives through Nickel(0)-Mediated [3 + 2] Cyclization of Alkenyl Fischer Carbene Complexes and Internal Alkynes. *J. Am. Chem. Soc.* **2007**, *129*, 14422-14426.

(4) (a) For a review of allylsilane [3+2] cycloadditions, see: Masse, C. E.; Panek, J. S. Diastereoselective Reactions of Chiral Allyl and Allenyl Silanes with Activated C=X π-Bonds. *Chem. Rev.* **1995**, *95*, 1293-1316. (b) Danheiser, R. L.; Carini, D. J.; Basak, A. (Trimethylsilyl)cyclopentene annulation: a regiocontrolled approach to the synthesis of five-membered rings. *J. Am. Chem. Soc.* **1981**, *103*, 1604-1606. (c) Danheiser, R. L.; Dixon, B. R.; Gleason, R. W. Five-membered ring annulation via propargyl- and allylsilanes. *J. Org. Chem.* **1992**, *57*, 6094-6097.

(5) (a) For a review of phosphine-based organocatalytic [3+2] cycloadditions, see: Methot, J. L.; Roush, W. R. Nucleophilic Phosphine Organocatalysis. *Adv. Synth. Catal.* **2004**, *346*, 1035-1050. (b) Sohn, S. S.; Rosen, E. L.; Bode, J. W. N-Heterocyclic Carbene-Catalyzed Generation of Homoenolates: γ-Butyrolactones by Direct Annulations of Enals and Aldehydes. *J. Am.*

Chem. Soc. **2004**, *126*, 14370-14371. (c) C. Zhang, X. Lu. Phosphine-Catalyzed Cycloaddition of 2,3-Butadienoates or 2-Butynoates with Electron-Deficient Olefins. A Novel [3 + 2] Annulation Approach to Cyclopentenes *J. Org. Chem.* **1995**, *60*, 2906-2908. (d) J.-C. Wang, S.-S. Ng, M. J. Krische. Catalytic Diastereoselective Synthesis of Diquinanes from Acyclic Precursors. *J. Am. Chem. Soc.* **2003**, *125*, 3682-3683. (e) White, N. A.; Rovis, T. Oxidatively Initiated NHC-Catalyzed Enantioselective Synthesis of 3,4-Disubstituted Cyclopentanones from Enals. *J. Am. Chem. Soc.* **2015**, *137*, 10112-10115.

(6) (a) Suzuki, K.; Urabe, H.; Sato, F. A Novel Tandem Cyclization of 2,7- or 2,8-Bis-Unsaturated Esters Mediated by (η^2-Propene)TiX_2 (X = Cl or O-i-Pr). A Facile Construction of Bicyclo[3.3.0]octane, -[4.3.0]nonane, and -[3.1.0]hexane Skeletons. *J. Am. Chem. Soc.* **1996**, *118*, 8729-8730. (b) Urabe, H.; Suzuki, K.; Sato, F. Intramolecular Cyclization of 2,7- or 2,8-Bis-unsaturated Esters Mediated by (η^2-Propene)$Ti(O\text{-}i\text{-}Pr)_2$. Facile Construction of Mono- and Bicyclic Skeletons with Stereoselective Introduction of a Side Chain. A Synthesis of *d*-Sabinene. *J. Am. Chem. Soc.* **1997**, *119*, 10014-10027.

(7) (a) Chowdhury, S. K.; Amarasinghe, K. K. D.; Heeg, M. J.; Montgomery, J. Diverse Reactivity Manifolds of Alkynyl Enone- and Alkynyl Enal-Derived Nickelacycles: Discovery of Nickel-Promoted [3+2] and [2+1] Cycloadditions. *J. Am. Chem. Soc.* **2000**, *122*, 6775-6776. (b) Amarasinghe, K. K. D.; Chowdhury, S. K.; Heeg, M. J.; Montgomery, J. Structure of an η^1 Nickel O-Enolate: Mechanistic Implications in Catalytic Enyne Cyclizations. *Organometallics* **2001**, *20*, 370-372. (c) Mahandru, G. M.; Skauge, A. R. L.; Chowdhury, S. K.; Amarasinghe, K. K. D.; Heeg, M. J.; Montgomery, J. Cascade Cyclizations and Couplings Involving Nickel Enolates. *J. Am. Chem. Soc.* **2003**, *125*, 13481-13485.

(8) (a) Hata, T.; Hirone, N.; Sujaku, S.; Nakano, K.; Urabe, H. Iron-Mediated Intramolecular Metalative Cyclization of α,β-Unsaturated Esters and Amides. Versatile One-Pot Preparation of Bicyclic Ketoesters. *Org. Lett.* **2008**, *10*, 5031-5033. (b) Hata, T.; Sujaku, S.; Hirone, N.; Nakano, K.; Imoto, J.; Imade, H.; Urabe, H. Iron-Mediated and -Catalyzed Metalative Cyclization of Electron-Withdrawing-Group-Substituted Alkynes and Alkenes with Grignard Reagents. *Chem. Eur. J.* **2011**, *17*, 14593-14682.

(9) (a) Herath, A.; Montgomery, J. Catalytic Intermolecular Enal−Alkyne [3 + 2] Reductive Cycloadditions. *J. Am. Chem. Soc.* **2006**, *128*, 14030-14031. (b) Li, W.; Montgomery J. Ligand-guided pathway selection in nickel-catalyzed couplings of enals and alkynes. *Chem. Commun.* **2012**, *48*, 1114-1116.

(10) (a) Jenkins, A. D.; Herath, A.; Song, M.; Montgomery, J. Synthesis of Cyclopentenols and Cyclopentenones via Nickel-Catalyzed Reductive Cycloaddition. *J. Am. Chem. Soc.* **2011**, *133*, 14460-14466. (b) Ohashi, M.; Taniguchi, T.; Ogoshi, S. Nickel-Catalyzed Formation of Cyclopentenone Derivatives via the Unique Cycloaddition of α,β-Unsaturated Phenyl Esters with Alkynes. *J. Am. Chem. Soc.* **2011**, *133*, 14900-14903.

(11) (a) Ahlin, J. S. E.; Donets, P. A.; Cramer, N. Nickel(0)-Catalyzed Enantioselective Annulations of Alkynes and Arylenoates Enabled by a Chiral NHC Ligand: Efficient Access to Cyclopentenones. *Angew. Chem. Int. Ed.* **2014**, *53*, 13229-13233. (b) Zhou, Y. Y.; Uyeda, C. Catalytic Reductive [4+1] Cycloadditions of Vinylidenes and Dienes. *Science*, **2019**, *363*, 857-862. (c) Farley, C. F.; Zhou, Y. Y.; Banka, N. Uyeda, C. Catalytic Cyclooligomerization of Enones with Three Methylene Equivalents. *J. Am. Chem. Soc.* **2018**, *140*, 12710-12714. (d) Zhou, Y. Y.; Uyeda, C. Reductive Cyclopropanations Catalyzed by Dinuclear Nickel Complexes. *Angew. Chem Int. Ed.* **2016**, *55*, 3171-3175.

(12) (a) Chang, H. T.; Jayanth, T. T.; Cheng, C. H. Cobalt-Catalyzed Diastereoselective Reductive [3 + 2] Cycloaddition of Allenes and Enones. *J. Am. Chem. Soc.* **2007**, *129*, 4166-4167. (b) Wei, C.-H.; Mannathan, S.; Cheng, C.-H. Regio- and enantioselective cobalt-catalyzed reductive [3+2] cycloaddition reaction of alkynes with cyclic enones: a route to bicyclic tertiary alcohols. *Angew. Chem. Int. Ed.* **2012**, *51*, 10592-10595.

(13) Williams, V. M.; Kong, J. R.; Ko, B. J.; Mantri, Y.; Brodbelt, J. S.; Baik, M.-H.; Krische, M. J. ESI-MS, DFT, and Synthetic Studies on the H_2-Mediated Coupling of Acetylene: Insertion of C═X Bonds into Rhodacyclopentadienes and Brønsted Acid Cocatalyzed Hydrogenolysis of Organorhodium Intermediates. *J. Am. Chem. Soc.* **2009**, *131*, 16054-16062.

(14) We also consider a pathway involving the direct insertion of benzaldehyde into the 5-membered metallacycle (labelled as pathway D). This pathway was found to be much higher in energy relative to the other 3 pathways, and is shown in the supporting information.

(15) Herath, A.; Li, W.; Montgomery, J. Fully Intermolecular Nickel-Catalyzed Three-Component Couplings via Internal Redox. *J. Am. Chem. Soc.* **2008**, *130*, 469-471.

(16) Shao, Y.; Gan, Z.; Epifanovsky, E.; Gilbert, A. T. B.; Wormit, M.; Kussmann, J.; Lange, A. W.; Behn, A.; Deng, J.; Feng, X.; Ghosh, D.; Goldey, M.; Horn, P. R.; Jacobson, L. D.; Kaliman, I.; Khaliullin, R. Z.; Kús, T.; Landau, A.; Liu, J.; Proynov, E. I.; Rhee, Y. M.; Richard, R. M.; Rohrdanz, M. A.; Steele, R. P.; Sundstrom, E. J.; Woodcock III, H. L.; Zimmerman, P. M.; Zuev, D.; Albrecht, B.; Alguire, E.; Austin, B.; Beran, G. J. O.; Bernard, Y. A.; Berquist, E.; Brandhorst, K.; Bravaya, K. B.; Brown, S. T.; Casanova, D.; Chang, C.-M.; Chen, Y.; Chien, S. H.; Closser, K. D.; Crittenden, D. L.; Diedenhofen, M.; DiStasio Jr., R. A.; Dop, H.; Dutoi, A. D.; Edgar, R. G.; Fatehi, S.; Fusti-Molnar, L.; Ghysels, A.; Golubeva-Zadorozhnaya, A.; Gomes, J.; Hanson-Heine, M. W. D.; Harbach, P. H. P.; Hauser, A. W.;

Hohenstein, E. G.; Holden, Z. C.; Jagau, T.-C.; Ji, H.; Kaduk, B.; Khistyaev, K.; Kim, J.; Kim, J.; King, R. A.; Klunzinger, P.; Kosenkov, D.; Kowalczyk, T.; Krauter, C. M.; Lao, K. U.; Laurent, A.; Lawler, K. V.; Levchenko, S. V.; Lin, C. Y.; Liu, F.; Livshits, E.; Lochan, R. C.; Luenser, A.; Manohar, P.; Manzer, S. F.; Mao, S.-P.; Mardirossian, N.; Marenich, A. V.; Maurer, S. A.; Mayhall, N. J.; Oana, C. M.; Olivares-Amaya, R.; O'Neill, D. P.; Parkhill, J. A.; Perrine, T. M.; Peverati, R.; Pieniazek, P. A.; Prociuk, A.; Rehn, D. R.; Rosta, E.; Russ, N. J.; Sergueev, N.; Sharada, S. M.; Sharmaa, S.; Small, D. W.; Sodt, A.; Stein, T.; Stück, D.; Su, Y.-C.; Thom, A. J. W.; Tsuchimochi, T.; Vogt, L.; Vydrov, O.; Wang, T.; Watson, M. A.; Wenzel, J.; White, A.; Williams, C. F.; Vanovschi, V.; Yeganeh, S.; Yost, S. R.; You, Z.-Q.; Zhang, I. Y.; Zhang, X.; Zhou, Y.; Brooks, B. R.; Chan, G. K. L.; Chipman, D. M.; Cramer, C. J.; Goddard III, W. A.; Gordon, M. S.; Hehre, W. J.; Klamt, A.; Schaefer III, H. F.; Schmidt, M. W.; Sherrill, C. D.; Truhlar, D. G.; Warshel, A.; Xua, X.; Aspuru-Guzik, A.; Baer, R.; Bell, A. T.; Besley, N. A.; Chai, J.-D.; Dreuw, A.; Dunietz, B. D.; Furlani, T. R.; Gwaltney, S. R.; Hsu, C.-P.; Jung, Y.; Kong, J.; Lambrecht, D. S.; Liang, W.; Ochsenfeld, C.; Rassolov, V. A.; Slipchenko, L. V.; Subotnik, J. E.; Van Voorhis, T.; Herbert, J. M.; Krylov, A. I.; Gill, P. M. W.; Head-Gordon, M. Advances in molecular quantum chemistry contained in the Q-Chem 4 program package. *Mol. Phys.*, **2015**, *113*, 184-215.

(17) Neese, F. Software update: the ORCA program system, version 4.0. *WIRES Comput. Mol. Sci.* **2019**, 8:c1327. doi 10.1002/wcms.1327.

(18) Chai, J.-D.; Head-Gordon, M. Long-range corrected hybrid density functionals with damped atom–atom dispersion corrections. *Phys. Chem. Chem. Phys.* **2008**, *10*, 6615-6620.

(19) (a) Hariharan, P.C.; Pople, J.A. The influence of polarization functions on molecular orbital hydrogenation energies. *Theoret. Chimica Acta*. 1973, *28*, 213-222. (b) Rassolov, V.; Pople,

J.A.; Ratner, M.; Windus, T.L. 6-31G* basis set for atoms K through Zn. *J. Chem. Phys.* 1998, *109*, 1223-1229.

(20) Lin, Y-S.; Li, G-D; Mao, S-P; Chai, J-D. Long-Range Corrected Hybrid Density Functionals with Improved Dispersion Corrections. *J. Chem. Theory Comput*., **2013**, *9*, 263-272.

(21) (a) Dunning, T.H. Gaussian basis sets for use in correlated molecular calculations. I. The atoms boron through neon and hydrogen. *J. Chem. Phys*. **1989**, *90*, 1007-1023. (b) Balabanov, N.B.; Peterson, K.A. Basis set limit electronic excitation energies, ionization potentials, and electron affinities for the 3d transition metal atoms: Coupled cluster and multireference methods. *J. Chem. Phys.,* **2006**, *125*, 074110.

(22) Marenich, A.V.; Cramer, C.J.; Truhlar, D.G. Universal Solvation Model Based on Solute Electron Density and on a Continuum Model of the Solvent Defined by the Bulk Dielectric Constant and Atomic Surface Tensions. *J. Phys. Chem. B*, **2009**, *113*, 6378-6396.

(23) Zimmerman, P. M. Single-ended transition state finding with the growing string method. *J. Comp. Chem*. **2015**, *36*, 601-611.

(24) (a) Zimmerman, P. M. Growing string method with interpolation and optimization in internal coordinates: Method and examples. *J. Chem. Phys*. **2013**, *138*, 184102. (b) Zimmerman, P. M. Reliable Transition State Searches Integrated with the Growing String Method. *J. Chem. Theory and Comp*., **2013**, *9*, 3043-3050.

(25) Wertz, D. H. Relationship between the gas-phase entropies of molecules and their entropies of solvation in water and 1-octanol. *J. Am. Chem. Soc.* **1980**, *102*, 5316-5322.